Available online at www.sciencedirect.com
ScienceDirect
Journal of Power Sources 162 (2006) 532–540
JOURNAL OF POWER SOURCES
www.elsevier.com/locate/jpowsour

Direct formic acid fuel cell portable power system for the operation of a laptop computer

Craig M. Miesse, Won Suk Jung, Kyoung-Jin Jeong, Jae Kwang Lee, Jaeyoung Lee*, Jonghee Han*, Sung Pil Yoon, Suk Woo Nam, Tae-Hoon Lim, Seong-Ahn Hong

Fuel Cell Research Center, Korea Institute of Science and Technology, 39-1 Hawolgok-dong, Seongbuk-gu, Seoul 136-791, Republic of Korea

Received 1 June 2006; received in revised form 6 July 2006; accepted 6 July 2006
Available online 15 September 2006

Abstract

A direct formic acid fuel cell (DFAFC) hybrid power system for a laptop computer has been developed at the Korea Institute of Science and Technology, Fuel Cell Research Center. At the heart of the system is a 15 MEA DFAFC stack capable of 30 W at 60 mW cm^{-2}. Stack characteristics relevant to integration into the power system such as concentration and orientation dependence, dynamic response, and long-term performance are elucidated and the resulting hybrid power system's performance is detailed. The stack's fast dynamic response eliminated the need for significant power buffering in the power conditioning equipment. The MEAs were found to give reduced but stable performance after 3 months of operation. The system is capable of an overall system efficiency of 0.23 (delivered power compared to theoretical power), and can operate under a substantial computing load for 2.5 h using a 280 mL tank of 50 wt.% fuel.

Keywords: Direct formic acid fuel cell; Fuel cell stack; Portable power supply; Dynamic response; Hybrid power system

1. Introduction

As the prevalence of portable electronic devices has increased dramatically in recent years, their functionality and operating times have coincidentally become limited by current battery technology. As well, better and longer performing portable power technologies are of immense importance for military operations. To meet the demands of next generation portable consumer electronics and wireless communication devices, the development of battery alternatives is of great interest. One prevalent technological approach to battery-replacement is the use of fuel cells to harness the immense energy density of liquid chemical fuels; nearly two orders of magnitude greater than that of the state-of-the-art secondary batteries [1]. Fuel cell systems offer other practical advantages over battery power systems, such as instant recharging via a replacement or a refilled fuel cartridge [2].

Fuel cells that use a proton conducting polymer electrolyte membrane are generally considered the best options as portable fuel cells. Such cells simultaneously catalyze the oxidation of hydrogen or a hydrogen-containing fuel and the reduction of oxygen to produce electricity. They produce primarily water and in some cases CO_2 as products and can use ambient air as an oxygen source. Traditionally, hydrogen-fed polymer electrolyte membrane fuel cells (PEMFCs) and direct methanol-fed fuel cells (DMFCs) are the dominant fuel choices for such cells. However, despite many years and billions of dollars of research into these technologies, inherent limitations remain. For PEMFCs, hydrogen is flammable and its low gas-phase energy density severely limits its practicality as a fuel for portable applications. Though schemes have been developed to compactly transport hydrogen as a constituent of other molecules such as ammonia, sodium borohydride, methanol, or hydrocarbons and subsequently catalytically generate hydrogen fuel on-demand, such approaches add cost, complexity, and bulk to the resulting fuel cell system or introduce other issues such as reduced cell performance and high temperature requirements that may be prohibitive for use in portable applications. Conversely, liquid methanol has an impressive energy density

* Corresponding authors. Tel.: +82 2 958 5277; fax: +82 2 958 5199.
E-mail addresses: jaeyoung@kist.re.kr (J. Lee), jhan@kist.re.kr (J. Han).

0378-7753/$ – see front matter © 2006 Elsevier B.V. All rights reserved.
doi:10.1016/j.jpowsour.2006.07.013

(approximately 4900 Wh L^{-1}), but its electrocatalytic oxidation rate lags severely behind that of hydrogen. Methanol's limited compatibility with the Nafion® membrane allows only low concentrations of methanol, generally 1–2 M, to be fed to a direct methanol fuel cell [3,4]. Exceeding this limit leads to a high rate of fuel cross-over, which simultaneously reduces fuel utilization and decreases cell performance. In addition to a number of other provisions, minimization of fuel cross-over requires either additional equipment (added bulk and system complexity) to dilute a concentrated fuel to an acceptable concentration, or simply the use of a dilute methanol fuel supply. The unacceptably low energy density of the latter approach wastes a key advantage for direct-liquid fuel cells. Regardless of whether these engineering problems are solved, methanol's inherent toxicity, particularly in the vapor phase, remains an issue for commercialization of DMFC technology [3]. This is an issue particularly relevant to larger systems, such as those in the power range of the system presented herein, because of the considerable amount of methanol vapor that is likely exhausted from the anode, carried by the produced CO_2, presumably to the environment.

It is these limitations of hydrogen and methanol that have in recent years increased interest in direct formic acid fuel cells (DFAFCs). Formic acid does not have many of the limitations of hydrogen and methanol. It is a non-flammable liquid at room temperature, naturally occurring, and a relatively benign chemical that is used as a food additive at lower concentrations [5]. In only a few years of very limited research, DFAFC technology has shown electrocatalytic oxidation activity far superior to DMFC and in some cases performance approaching that of PEM fuel cells [6]. Formic acid's well-known dual-pathway electrocatalytic oxidation mechanism [7] can be tuned to pass predominantly through the favored dehydrogenation pathway, reducing the kinetic encumbrance by CO poisoning seen in DMFC and reformate fed PEMFCs [6,8]. The rate of formic acid cross-over is considerably less than that of methanol, allowing for high fuel concentrations and thinner electrolytes [8–10]. The major disadvantage of formic acid as a fuel is that its volumetric energy density is 1870 Wh L^{-1} (HHV), considerably lower than that of neat methanol. For many systems, especially smaller systems, the advantages of DFAFC can outweigh those of its primary direct-liquid fuel cell contender, DMFC.

The system described in this paper is a hybrid system. To meet the power demands of a laptop computer, an actively fed fuel cell stack is required. Hence, a miniature liquid fuel pump and a miniature air compressor and other components are necessary, requiring a small battery to drive these components during system start-up. Recently, many electronics companies have announced similar hybrid system developments, all powered by DMFC stacks [11].

The purpose of this paper is to present the accomplishments made in the development of a 30 W portable direct formic acid hybrid power system. The design aspects and fundamental and operational performance results of the fuel cell stack and the integrated hybrid device will be presented and discussed. Among the results, the first reported dynamic response of a DFAFC system will be presented. Further developments required to enable commercialization will be discussed.

2. Experimental and system design

2.1. MEA fabrication

Catalyst ink was prepared by sonication of water, small-chain alcohols, ionomer solution, and catalyst powder (PtRu for anode, Pt black for cathode) as-received from Johnson-Matthey. To prepare the electrodes, carbon cloth (E-Tek) that was previously treated with a thin layer of PTFE, carbon black, and glycerol, was coated with a relatively thin layer of ionomer solution, a relatively thick layer of ink, and finally another relatively thin layer of ionomer solution. The thin layers of ionomer solution are employed to increase the area of the triple-phase boundary. Catalyst loading for both anode and cathode was 3 mg cm^{-2}. The fabricated electrodes were dried at 80 °C for at least 1 h and subsequently hot-pressed to either side of a piece of pre-conditioned Nafion® 115. The resulting MEAs had active electrode areas of 32.6 cm^{-2}.

2.2. Stack

Fifteen MEAs were stacked in series, separated by bipolar plates (BPPs), and bolted between endplates. The stack had internal manifolds which fed either air or formic acid to each MEA in parallel. The BPPs had square-grooved, parallel, serpentine flow-fields. Fig. 1a shows the stack design. The stack had an 88 mm × 70 mm footprint and the 1.5 mm pitch BPPs were composed of a graphite-composite material. To reduce stack and system volume, current collectors were abandoned in favor of copper lead wires that were inserted into the terminal, one-sided flow-fields, also composed of the graphite-composite material. Eight bolts evenly distributed the force of the endplates on the stack. Two 40 mm × 40 mm cavities were machined on the middle of the exterior of the endplates and copper heat sinks were attached with two-sided thermally conductive tape (3 M). The stack's dimensions were 88 mm × 70 mm × 50 mm for a total volume of 308 cm^3. Its weight was 0.65 kg.

After the stack was assembled, two leak tests were performed. The first test consisted of pressurizing the inside of the stack to 0.5 bar and checking for leaks at the gaskets and any other potential leak locations with a leak-detection solution known not to contaminate Nafion® membranes. If no exterior leaks were detected, an interior leak test was performed to verify seal

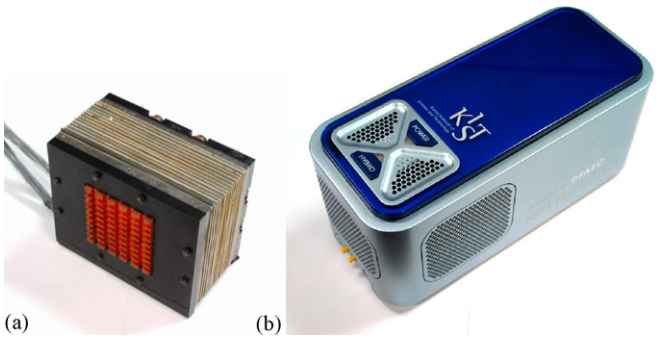

Fig. 1. (a) Image of the stack design. (b) Image of the hybrid power system.

Table 1
Stack and system size and performance specifications

	Dimensions (cm)	Volume (cm^3)	Weight (kg)	Standard output[a]	Standard output efficiency	Maximum output (W)
15 MEA stack	$8.8 \times 7.0 \times 5.0$	308	0.65	21 W @ 6.75 V	0.35[b]	45
Hybrid system	$20.5 \times 8.5 \times 8.25$	1440	1.8[c]	13.7 W @ 12 V	0.23[d]	–

[a] Assumes a substantial computing environment, such as multiple programs operating and with USB devices attached.
[b] η_{stack} as defined in text.
[c] Assumes a full fuel tank.
[d] η_{SYSTEM} as defined in text.

integrity between the anode and cathode chambers inside the stack. For this test, one side of the stack (anode or cathode) was pressurized to 0.5 bar while the other side was connected to a tube submerged in water. Observation of bubbles indicated a bad seal, generally requiring disassembly, troubleshooting, and reassembly. Different gasket materials were screened to determine the optimum combination of gasket thickness, hardness, chemical compatibility with formic acid, and bolt torque. Using PTFE gaskets at low torque provided the most reliable internal seal between anode and cathode ducts inside the stack. Gasket materials are summarized in Table 1.

Prior to stack operation with formic acid, a two-step pretreatment process was performed to condition the MEAs. First, the MEAs were hydrated by circulation of hot water on both the anode and cathode. This was followed by methanol conditioning, shown to enhance DFAFC performance [12].

Stack performance tests were performed using a liquid and gas distribution system set to feed rates similar to those provided to the stack in the integrated system. Polarization curves were measured using a loader that was manufactured in-house, and measured using either a digital voltmeter or a Daqstation DX106 acquisition system manufactured by Yokogawa Electric Co. Individual MEA potentials were recorded manually using a digital voltmeter for further analysis. Dynamic response measurements were performed using a programmable DC loader, model UDL-300 manufactured by Unicorn Co., Ltd., and recorded using the Yokogawa recorder.

2.3. Hybrid system

The stack described above was packaged in a case that included a fuel tank, tubing, and the five major balance of plant (BOP) components: a miniature liquid pump, a miniature air compressor, cooling fans, a small battery, and a power conditioning control board (PCB). Fig. 1b shows the packaged, integrated system.

In the current design generation, the fuel tank starts with concentrated formic acid that is simply circulated directly to the stack in a loop. Fuel is drawn from the bottom of the fuel tank, pumped to the anode chamber of the stack where a small amount is reacted. The anode exhaust stream is returned to the top of the fuel tank with entrained CO_2 produced during the electrocatalytic oxidation of formic acid at the anodes. A gas–liquid separator at the top of the fuel tank exhausts the CO_2 to the environment and returns the remaining formic acid to the tank. Over the lifetime of the tank, the concentration of the fuel gradually decreases. This approach is not optimal for stack performance, and will be discussed along with an alternative design in a later section of this paper.

Ambient air was supplied to the fuel cell stack by a rotary-vane compressor (Rietschle-Thomas G 12/04 EB). The measured flow rate of the compressor through the 15 MEA stack and tubing was 4.6 L min^{-1}. Air exhausted from the stack was returned to the room.

Formic acid was pumped from the fuel tank to the stack by a miniature diaphragm pump (KNF NF5). The measured flow rate of the liquid pump through the 15 MEA stack and tubing was 26 mL min^{-1}. It should be noted that the optimum formic acid flow rate depends on concentration and that increasing the flow rate generally resulted in decreased cell performance.

Three cooling fans were mounted in the system case and forced ambient air to the cooling fins on the endplates and out vents in the side of the case. System heat removal was focused at the stack because it is the location of the majority of the heat generation, and because excessive internal temperature can have a deleterious effect on MEA stability.

Though the stack is capable of easily meeting a laptop's power demands, as stated in Section 1, a small battery was included in the system as a power source to start the system. After the stack has reached steady-state, it recharges the battery, and generates all of the power for the BOP and laptop computer. The charged battery also plays a role in power conditioning during system operation.

The PCB conditions and distributes the power received from the stack (approximately 20 W at 6.5 V) to the BOP and to the attached laptop computer. It supplies power to the laptop, the liquid pump, and air compressor, and charges the battery. A resistance temperature detector attached to the stack signals the PCB to supply power to the cooling fans when the stack exceeds 50 °C. The PCB also includes capacitors to function as a buffer between the laptop's rapidly changing power demands and the stack's relatively slower response.

The case that houses all of the system components described above (Fig. 1b) encloses a volume of 20.5 cm × 8.5 cm × 8.25 cm (1438 cm^3). The total system weight, with and without fuel is 1.5 kg and 1.8 kg, respectively. Key stack and system specifications are given in Table 2.

The performance of the hybrid power system is tested with an actual laptop computer. The standard 12 V battery that is removed from the laptop prior to operation with the hybrid power system is 95 cm^3, with a weight of 0.16 kg. Thus, the net volume and weight increase of the power system is 1343 cm^3 and 1.64 kg.

Table 2
Gasket materials

Base material	Sealing integrity	Compatibility with formic acid	Other considerations
Low durometer silicone	No	Medium	Failure under medium compression
PTFE	No	High	
Glassy epoxy	No	Low	Gasket is difficult to manufacture
PTFE-coated epoxy	No	High	Gasket is difficult to manufacture
High durometer silicone	Yes	Medium	
Epoxy-silicone	Yes	Medium	Gasket is difficult to manufacture
PTFE	Yes	High	

The hybrid power system's performance was tested by the laptop computer using a full tank of 50 wt.% formic acid. A Yokogawa digital data recorder was used to record voltages and temperatures during the system performance measurements.

3. Results and discussion

3.1. Stack

Though in recent years the interest in DFAFC technology has increased, to date, no results from a stack have been published. Two potential complications that are introduced as a result of stacking DFAFC MEAs in series are fuel distribution and possible polarization by the aqueous fuel that forms a continuum between all of the cells and bi-polar plates. With regard to the former concern, the performance of individual MEAs in a stack was measured. The MEAs were then shuffled to new positions and performances were measured again. No correlation was evident between an MEAs' position in the stack and its performance, validating the effectiveness of the fuel distribution methods of both formic acid and air. Liquid fuel distribution can become an issue if the stack orientation is altered. This will be explored later in the text. The latter concern is raised because formic acid's electrical conductivity is significantly higher (approximately 4 orders of magnitude) than that of methanol, the traditional fuel used in direct-liquid fuel cell stacks. Formic acid has been predicted to facilitate significant electronic transport within a fuel cell's anode compartment [13]. Such electronic transport would be prohibitive to a practical fuel distribution method such as that employed in our design. Yet, the conductivity of formic acid, though high relative to methanol, is still small when compared to that of a metallic conductor (yet another 4–5 orders of magnitude higher), and experiments verify that the performance of the stacked MEAs is in line with that of their individual single-cell performance.

One of the reported advantages of a direct formic acid fuel cell is the ability to give consistent performance from a wide fuel concentration range. Zhu et al. have demonstrated this trait specifically for the same anode and cathode catalysts employed in this study [14]. This trait would be very beneficial to the system because, as described in Section 2.3, the concentration fed to the stack varies significantly over the course of operation. Fig. 2 shows the downward polarization curves of the stack operated with a range of formic acid concentrations. The optimum concentration appears to be around 6 M and, as the concentrations deviate from the optimum, performance drops consistently. Though the 6 M performance was comparable at the target operating range, the concentration dependence was not as favorable as reported by Zhu et al. The low performance of the 3 M trial is believed to be caused by mass-transfer limitations. The decrease in performance with increasing concentration is believed to be caused primarily by cross-over of the formic acid to the cathode. This was supported by the temperature profiles of these experiments. Both the OCV temperature and the rate of cell temperature rise increased with concentration, indicating that cross-over was becoming more pronounced. The differences between the measured concentration dependence in Fig. 2 and that of Zhu et al. may be due to the varying methods of gas-diffusion layer (GDL) preparation, catalyst layer composition, MEA fabrication, and pre-conditioning, as these factors can play large roles in cross-over [15,16].

The polarization curves in Fig. 2 show a much earlier onset of the mass-transfer limitation than Zhu et al.'s data. This is easily attributed to the relatively low flow rates of the fuel and oxidant used in the stack measurements. To attain data from the stack that was relevant to system integration, flow rates corresponding to the capacities of the system's liquid pump and air compressor were chosen. Thus, the MEA surface area-normalized flow rates of the fuel and air were just 20% and 12%, respectively, of those used in Zhu et al.'s experiments.

Because of the portable nature of a laptop computer, effects of orientation on stack performance are of interest. The impact

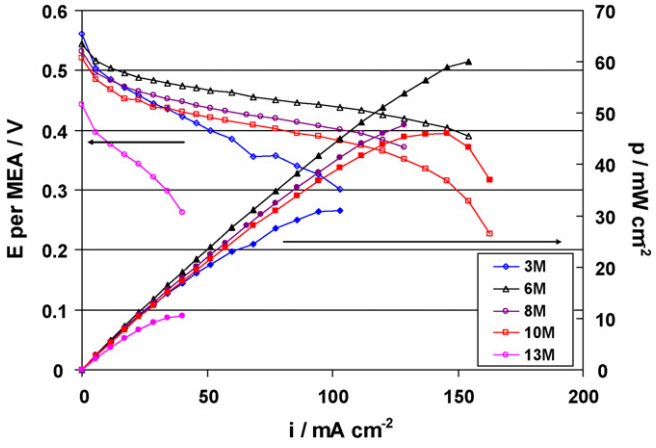

Fig. 2. Effect of formic acid concentration on performance. Data were taken for five distinct concentrations. Dry air was fed at 4500 sccm to the cathode, and 6 M formic acid was fed to the anode at 21 mL min^{-1}.

of CO_2 accumulation, in particular, is expected to be a key factor in the effect of orientation. The stack, as stated, had internal feed manifolds for both the air and liquid feeds. Inlet and outlet conduits for both the anode and cathode chambers were on the same side of the stack, penetrating one endplate. Three stack orientations were tested. The first orientation saw the stack standing on the smallest end (the 70 mm × 50 mm end), with the MEAs orthogonal to the table. This orientation was expected to be optimal because the formic acid is fed into the bottom of each cell's flow-field (giving best-case wetting of the anode GDL) and because CO_2 generated at the anode needs only to travel either horizontally or up (in the direction of the buoyant force) in order to be exhausted from the flow-fields. The second orientation saw the stack sitting on the longer side (the 88 mm × 50 mm end), with the MEAs orthogonal to the table. This was similar to the first in that the formic acid feed was into the bottom of each cell's flow-field. But, for this orientation, generated CO_2 bubbles were required to travel down the flow-fields multiple times. The final orientation saw all conduits pointing down, with the MEAs parallel with the table. Fig. 3 shows the downward polarization curves of the three different designs. It should be noted that to insure CO_2 was generated in amounts sufficient to show an effect, the data points were taken at 90 s intervals. The performance of the first two orientations were practically identical, suggesting that the need for CO_2 bubbles to travel down the flow-field grooves is not a factor in performance. The third orientation, however, severely hampered the stack's output. This decreased performance is believed to be caused by some combination of accumulation of CO_2 and poor liquid fuel distribution. In the first two orientations, the exit point for the formic acid and CO_2 was at the top end of the stack. For the third orientation, the exit point was at the bottom of the stack. While the results of the first two orientations showed that CO_2 is capable of avoiding accumulation by traveling downward in the individual flow-fields of each stacked cell, it is likely that in the third orientation, the CO_2 can more easily accumulate and rise to the top end (opposite end of the exhaust) of the stack once it leaves the flow-field channel and enters the larger, downward flowing

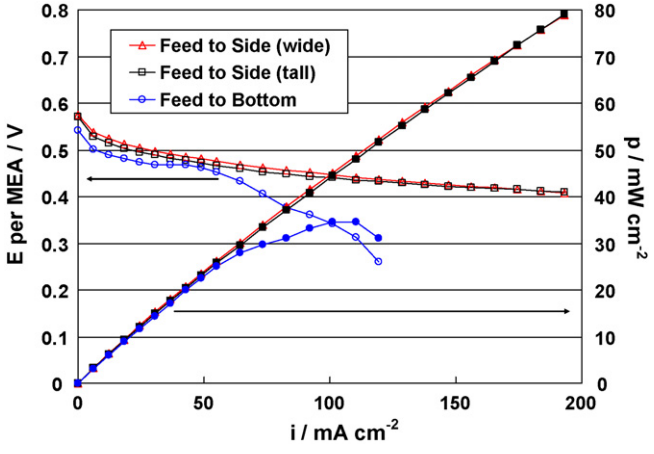

Fig. 3. Effect of stack orientation on performance. Data were taken for three distinct orientations. Dry air was fed at 5000 sccm to the cathode, and 6 M formic acid was fed to the anode at 25 mL min^{-1}.

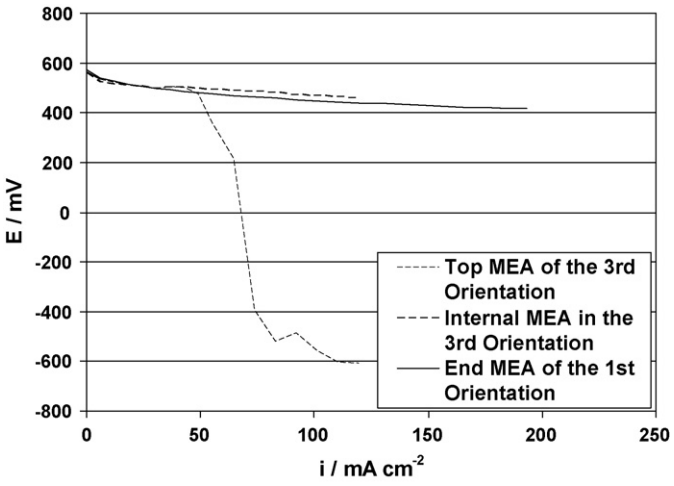

Fig. 4. Effect of MEA position with orientation. For the third orientation as defined in the text, comparison of the performance of the top MEA and an arbitrarily selected internal MEA shows the effect of CO_2 accumulation and poor fuel distribution on the top MEA. In the first and second orientation, the same MEA, denoted as the "End MEA" in the plot legend, showed performance similar to that of the mean of all MEAs.

manifold. Regarding fuel distribution in this orientation, equal liquid fuel distribution to each MEA is not as likely for fuel can very easily short-circuit the upper MEAs by favoring the lower-lying MEAs. These two problems should have the greatest effect on the top MEAs of the stack. Indeed the effect of some combination of the two problems was supported by measurements of individual MEA potentials during the stack polarization experiment. Specifically, the performance of the topmost MEA was the first to show a significant and prolonged performance decrease in the third orientation. In Fig. 4, the data series that are depicted with broken lines are data from the polarization curve for the third orientation, and compares the drastic performance drop of the topmost MEA to the performance of an arbitrarily selected internal MEA from the same experiment. The solid line in Fig. 4 represents the performance of the same MEA when the stack is in the first orientation. It shows that unlike its performance in the third orientation, this MEA has a polarization curve similar to that of the other MEAs in the stack when the stack is in the first orientation. The individual MEA potential measurements of the first two orientations showed no dependence on position or time.

3.2. Dynamic response

The power demands of portable electronics devices vary during their operation. For example, for a mobile phone, the demand varies drastically, particularly when placing or receiving a call. Laptops, conversely, have relatively steady power demands, incurring spikes when programs are launched, documents are opened, USB peripherals are attached, etc. These spikes range between 10% and 40% of the baseline operation power demand. Transient response data from a direct formic acid fuel cell or stack have not been reported in literature, but are an important characteristic and relevant to the design of a system's power conditioning.

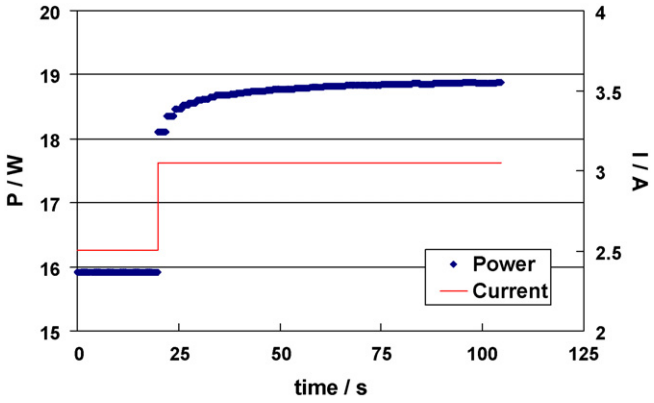

Fig. 5. Transient response of the 15 MEA stack to a step-change in current. Formic acid (6 M) was fed to the anode at 26 mL min^{-1} while 4600 sccm of dry air was fed to the cathode. The stack temperature was 45 °C.

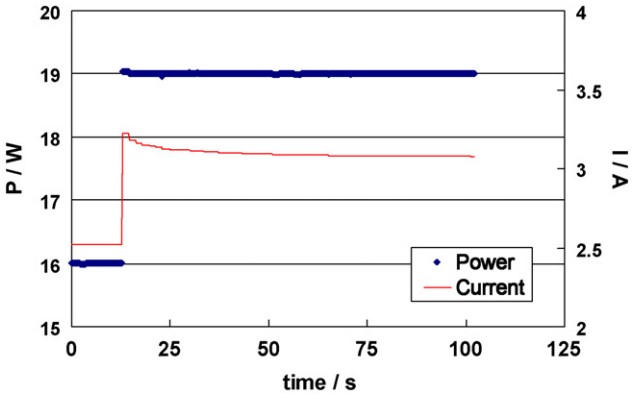

Fig. 6. Transient response of the 15 MEA stack to a step-change in power demand. Formic acid (6 M) was fed to the anode at 26 mL min^{-1} while 4600 sccm of dry air was fed to the cathode. The stack temperature was 45 °C.

When a sudden load change occurs in a direct-liquid fuel cell, there are many interdependent factors that can affect the cell's response characteristics, for example, anode and cathode catalytic activities, interfacial capacitance within the MEAs, multi-phase and multi-directional mass transport of reactants and products through the diffusion layers and catalyst layers of both electrodes, and fuel cross-over [17,18]. Argyropolous et al. have determined that for DMFCs, the mixed potential caused by methanol cross-over was a significant cause of a sluggish response [19]. Formic acid's superior kinetics and cross-over characteristics make a comparative dynamic response study attractive. In this paper, however, the focus of the dynamic response experiments is to determine the need for supplementary power system components, such as capacitors, to act as a buffer between the relatively slow stack response and the quicker demand changes of the laptop.

Two types of dynamic response data were taken for the 15 MEA stack. For the first type, shown in Fig. 5, the programmable loader gave a step-change in current (76.7–93.5 mA cm^{-2}) that corresponds to a change in steady-state stack output power of 16–19 W. This change (16–19 W) is characteristic of an extreme but possible power demand change on the stack by the rest of the system when operating the laptop computer. After the step-change, the voltage (and power) was allowed to equilibrate while the current was held constant. The second dynamic response data, shown in Fig. 6 were taken by programming the loader to demand a step-change in power, again 16–19 W. After the step-change, the voltage and current were allowed to equilibrate while the power drawn from the stack was constant. Making the assumption that the responses of each MEA in the stack are quite similar, the response shown can be viewed simply as a 15× amplification of a single MEA's response.

The response to the step-change in current resulted in an initial drop in voltage of 431 mV (from 6.363 V to 5.932 V), 248 mV less than the final steady-state voltage (6.180 V), and corresponding to 18.1 W. It took 64 s to recover 95% of initial voltage loss below the final steady-state value. If the load profile shown in this experiment was representative of a realistic load change for the stack, approximately 6.8 J of energy would be provided by auxiliary power equipment (battery and/or capacitors) to meet the power demands as the stack progresses through the transient. Fortunately, a step-change in current is not a realistic situation.

The response depicted in Fig. 6 is a realistic simulation of the actual load change that the stack encounters when connected to the system and laptop, and therefore can be used for power conditioning system design purposes. It is apparent that the stack can react very quickly to meet a step-change in power demand. In fact, no power lag was detected by the recorder (resolution of 200 ms). Because of the aforementioned factors, there was an initial the drop in the output voltage and increase in current. Interestingly, the voltage recovery profile attained from a step-change in power demand was nearly identical to the recovery profile of the current step-change. The initial drop in voltage was 445 mV (from 6.350 V to 5.905 V), 271 mV less than the final steady-state voltage (6.176 V). It took 65 s to recover 95% of initial voltage loss below the steady-state value. At the level of resolution of the recorder (200 ms), there was no need detected for auxiliary power equipment to act as a buffer between the power demands of stack and its transient response, though over a smaller time scale, certainly some lag existed. Additionally, from a system point of view, the power conditioning circuitry is likely to require a certain amount of buffering during a transient, as it must supply the BOP and laptop power with constant voltage power output despite receiving a sudden change in input voltage and current from the stack.

3.3. Long-term MEA stability

To be a commercially viable, a fuel cell system must show stable long-term performance. In Nafion®-based fuel cells, there are many known factors that cause performance degradation to MEAs [20–22]. To determine the long-term performance endurance of MEAs produced using the procedure in Section 2.1, 3 months of performance data were recorded and are shown in Fig. 7. The data were taken at a current density of 92 mA cm^{-2}. The five upward spikes in voltage were realized immediately after resource outages that occurred during the 3-month test. The first four spikes were caused by laboratory electrical blackouts, which cut feed to both the anode and

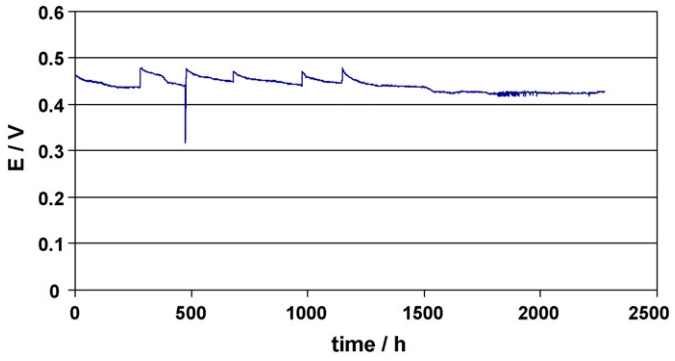

Fig. 7. Plot of long-term single-cell MEA performance. The five upward spikes in voltage were caused by resource outages that occurred during the 3-month test. During the test, the cell was maintained at 60 °C. Six molar formic acid was fed to the anode at 5 mL min^{-1} and 250 sccm of humidified oxygen was fed to the cathode.

cathode. The final spike coincided with a temporary oxidant supply outage.

Three main observations can be made from Fig. 7. The first observation is that the output was relatively stable after approximately 3 months of nearly continuous operation. The second is that despite the initial performance degradation exhibited after the initiation of the test as well as each restart, a steady-state value is reached after several hundred hours under a continuous load. The final observation was revealed by the experimental problems that occurred during the test. The initial performance degradation can be recovered, giving a voltage similar to the initial voltage.

Many mechanisms for performance degradation in fuel cells using Nafion® membranes have been proposed, particularly for irreversible degradation. These include catalyst sintering, catalyst loss and migration, electrode and membrane contamination, increases in the membrane resistance, decreases in species mass transfer in the MEA, and can be interrelated [21,23–25]. Of particular interest is the observation of performance recoverability. Although the DMFC performance degradation tests of Xie et al. were substantially shorter in duration, they showed the identical observation that performance can be recovered to near the initial level by stopping the flow of oxygen to the cathode. Though no in-depth analysis of the regeneration mechanism was performed, Xie et al. suggest that the recovery process depends on the relative potential of the cathode and anode [25]. Ha et al. have shown that for a DFAFC using Pd black as an anode catalyst, briefly applying a 1.0 V versus DHE anodic potential can regenerate the majority of the lost performance [5]. Thus, these observations of performance recoverability are possibly due to reversible catalyst poisons that are cleaned from the surface when the appropriate potential is applied.

The ability to regenerate performance suggests an opportunity of developing engineering methods to maintain higher performance even under long-term operation. An example of such a scheme is given by Xie et al. [25]. It also suggests that cycling a cell or stack, as would occur routinely with a system such as that currently described, can help recover a cell's or stack's decreased performance.

3.4. Integrated system

After successful development of a fuel cell stack capable of producing 30 W at 6 V (~60 mW cm^{-2}), the stack and other components described in Section 2.3 were integrated to create the hybrid power source.

The hybrid fuel system's operation time provided by one full tank of fuel is a primary characteristic. The system was operated with 280 mL of 50 wt.% (11 M) formic acid for approximately 150 min. During this test, depicted in Fig. 8, the laptop computer was booted, the screen brightness was set to a comfortable setting, and a medium computational load was set up to provide an above average draw by the computer throughout the test.

The voltage trend plotted in Fig. 8 has three main regions: start-up, standard operation, and fuel-depletion. The system and the computer are both started at time zero. During system start-up, the battery is used to boot the system while the stack voltage slowly falls to the steady-state OCV. When reaching a value slightly above 8 V, the PCB begins to draw current from the stack, which corresponds to the sudden voltage drop at 5 min. At this time, the screen brightness is adjusted and the computational load is launched. During the standard operation period, the voltage steadily rises, corresponding to the steady decrease in fuel concentration. Because the load remains quite constant throughout the test, this steady increase in stack voltage is attributed to a decrease in fuel cross-over. In the final region of the voltage trend, the voltage turns quickly downward, corresponding to depletion of fuel. The on-board battery, which was recharged by the stack after its use in the first 5 min of the test to boot the computer, then powered the laptop for the remainder of the test. The final formic acid concentration was 2.1 M. Thus 81% of the original 11 M fuel was consumed before mass-transfer limitation at the anode was detrimental to stack's ability to supply the required power. Without the battery, the stack and fuel provided slightly over 2 h of power to the laptop.

Fig. 8 also shows the stack temperature profile of the operation cycle. The total active electrode area in the 15 MEA stack is nearly 500 cm^2. At the targeted operating conditions

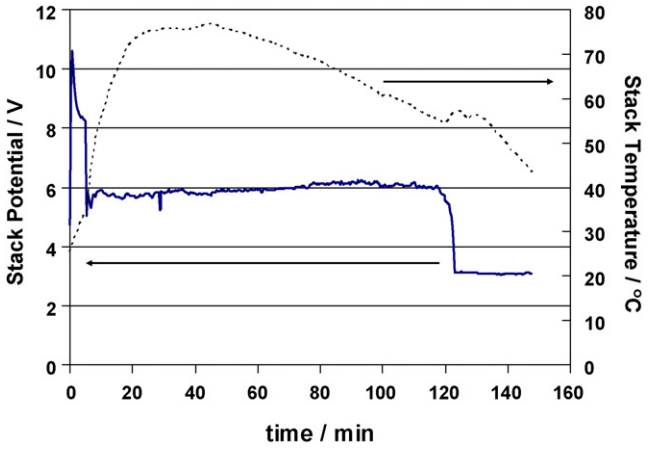

Fig. 8. Hybrid system performance for a single operation cycle using 280 mL of 11 M formic acid (approximately 50 wt.%). Stack temperature was measured by a thermocouple placed inside the cathode current collector.

of 0.4 V/MEA at 150 mA cm^{-2}, an estimated 70 W of waste heat is generated in the stack. Much of this heat is transferred to the formic acid as a sensible heat change and retained in the system. Thus, thermal management is an important design consideration. The design goal was to maintain a cell temperature at or below 60 °C. As can be seen, however, the stack temperature exceeds the target throughout the majority of the operation. This was somewhat of a surprise because design calculations and a thermal design experiment carried out on a prototypical system demonstrated the effectiveness of the three cooling fans at maintaining the stack temperature below 60 °C. The structural differences between the prototype and final design, made for aesthetic purposes, such as smaller fan ports and relocated case exhausts, therefore were the cause of the system's thermal operating profile.

System efficiency measurements were made by comparing the power demands of the laptop computer, the BOP components, the power output of the stack, and the amount of formic acid converted. Efficiency can be conveniently divided into two terms, whose product is the overall system efficiency, η_{SYSTEM}. The first is stack efficiency, which is defined as:

$$\eta_{STACK} = \frac{P_{stack}}{P_{theoretical}} \quad (1)$$

where P_{stack} is the amount of power transferred from the stack to the PCB, and $P_{theoretical}$ is the theoretical power available (based on the fuel's HHV) for the rate of formic acid consumption. The second is the BOP efficiency, defined as:

$$\eta_{BOP} = \frac{P_{net\ output}}{P_{stack}} \quad (2)$$

where $P_{net\ output}$ represents the power available to the laptop computer. This term will include the losses caused by the requirements of the miniature liquid pump and air compressor, cooling fans, battery charging, and the power conditioning of the PCB.

The stack efficiency was affected by many factors, such as the power demand, formic acid concentration, temperature, and to a lesser extent from variations in the MEAs used to construct the cell. As a result, it is not possible to give a definitive value for the stack efficiency. Hence, an estimate at reasonable operating conditions will be discussed. A conservative value of the power requirement of the stack to operate the BOP and laptop is approximately 21 W. At this load, with 6 M fuel and a temperature of ~60 °C, η_{STACK} was 0.35.

As is evident by Fig. 2, concentration will have a large effect on this efficiency. At higher concentrations, cross-over will reduce the efficiency. Cell temperature showed a smaller but considerable effect. An efficiency increase of about 0.02 consistently occurred during the polarization tests when the cell temperature rose just above 40 °C, though the mechanism for this performance enhancement was not investigated.

The work presented herein is a development project, and many opportunities to improve stack efficiency exist. The miniature pumps and air compressors used were the best choice among off-the-shelf models, but were not optimized for their purpose. The air compressor was undersized, though it is not certain if the increased stack efficiency resulting from a greater air flow rate would justify the increased power demand of a larger compressor. Also, MEA fabrication processes and materials, including catalyst composition and preparation, GDL composition, cell conditioning, etc., have not been optimized. More active formic acid electro-oxidation catalysts have been developed that have the potential to yield much better performance [5,6,26].

The BOP efficiency (η_{BOP}) was simply determined by directly measuring the power demand of the laptop computer and comparing it to the measured power requirement of the laptop and all of the BOP components. These measurements were made over a range of computing tasks, and were all within a few percentage points of the average $\eta_{BOP} = 0.65$. No trend between laptop power demand and BOP efficiency was statistically evident. Direct measurement of the power demands of the BOP components made under realistic operating conditions showed that the largest sources of loss were the power conditioning components. A total of 3.8 W of the power from the stack is consumed by the power conditioning components in order to supply power to the system components and attached laptop. This value is nearly as much as the total power demand of all of the other components combined (air compressor at 2.2 W; liquid pump at 0.14 W; cooling fans at 0.60 W each). The conversion efficiency of the power conditioning equipment is 0.88. This value is simply the fraction of the stack's output power that is passed on for the operation of the air compressor, liquid pump, cooling fans, battery, and laptop. Hence, 12% of the stack's power output is lost outright by power conditioning.

As in the case of the stack's efficiency, opportunities exist for η_{BOP} improvement. Most importantly, improvements to the sophistication of the power conditioning system could reduce the system's dominant loss. Improvements in stack efficiency have a synergistic effect on the BOP efficiency as well, as a more efficient stack will generate less heat, reducing the cooling fan duty. A more efficient stack will operate at a higher voltage, which will yield higher conversion efficiency by the PCB.

Combined, the stack and BOP efficiencies give an estimated overall system efficiency of 0.23. This is at par with the system efficiency achieved by Xie et al. [25] for a miniature DMFC power system. Using Eqs. (1) and (2), their DMFC system efficiency was 0.19.

The most beneficial improvement that can be made for the system is adding a method to control the concentration of the formic acid fed to the stack. The current fuel-delivery system, a circulating loop between the fuel tank and the stack, greatly limits the performance of the system. Ideally, concentrated formic acid from the fuel tank should be metered into a smaller, circulating fuel loop at a rate that maintains the fuel loop at the concentration that yields maximum performance. Such a scheme has many advantages. Of course operating at the optimum concentration maximizes stack efficiency. Overheating and reduced fuel utilization due to the cross-over that occurs when the higher formic acid concentrations are fed to the stack will be eliminated. Currently, to prevent overheating, the maximum allowable formic acid concentration in the feed is approximately 50 wt.%; hence, the concentration control system will double the system's energy density by enabling pure formic acid to be used

in the tank. The circulating stream will be cooler and, on average, at a lower concentration than in the current design, thereby reducing the formic acid emissions that leave with the generated CO_2. The cost of fuel concentration control is the complexity and volume that the additional instrumentation (at least a sensor and another liquid pump) adds to the system. Feed loop concentration control is possible only via a reliable concentration measurement method. Controlling the injection of formic acid into the stack's fuel supply loop will require a reliable concentration sensor. Measuring pH is an attractive option as pH shows reasonable sensitivity to formic acid concentration. Controlling concentration by measuring conductivity is not a likely solution because formic acid's conductivity is not an injective function with concentration, and does not show a sufficient sensitivity in the target concentration range. Another alternative is to employ an electrochemical sensor such as that described in Ref. [27].

The development of hybrid power systems for laptops using DMFC technology has been announced by several electronics companies. However, these prototypes were not reported in peer-reviewed scientific journals, so technical data are limited to what was included in their respective press releases. Thus, a rigorous and accurate comparison is not possible. These hybrid power systems generally had similar or slightly larger volumes and advertised between 10 h and 15 h of operation with 200–300 mL fuel tanks, which compare favorably to the system detailed in this paper. Implementing the design improvements described above can be reasonably expected to extend the single-tank operation time of the DFAFC system to approximately three times the current time (a two-fold enhancement will be afforded solely by doubling the initial fuel concentration).

4. Conclusions

The development of a prototypical hybrid direct formic acid fuel cell power supply for a laptop computer has been presented. A 15 MEA DFAFC stack capable of producing 30 W at 60 mW cm^{-2} was developed and its performance characteristics relevant to system integration were described. The dynamic response of the stack was sufficiently fast that only a small amount of supplementary power storage is necessary to meet the transient power demands of a laptop computer. The hybrid system successfully operated a laptop computer for over 150 min using 280 mL of 50 wt.% formic acid. Optimal system efficiency was 0.23, though when higher concentrations of formic acid were used, it was considerably less. Analysis of the system performance has yielded design recommendations that should improve system efficiency and extend the operation time of the next-generation system an estimated three-fold. The many performance improvements that were made and suggested during the reported development are substantial; however, many technical challenges, for example, lifetime and cost, must be solved before such a system is ready for the consumer market.

Acknowledgements

This work was supported by the Korean Institute of Science and Technology. The authors would like to thank Mr. Sungryel Choi for his assistance in system packaging design.

References

[1] A.C. Fernandez-Pello, Proc. Comb. Inst. 29 (2003) 883–899.
[2] S. Ha, Z. Dunbar, R.I. Masel, J. Power Sources 158 (2006) 129–136.
[3] J. Larminie, A. Dicks, Fuel Cell Systems Explained, John Wiley & Sons Ltd., Wiltshire, 2003.
[4] H.J. Kim, T.H. Lim, J. Ind. Eng. Chem. 10 (2004) 1081–1085.
[5] S. Ha, Y. Zhu, R.I. Masel, Fuel Cells 4 (2004) 337–343.
[6] Y. Zhu, Z. Khan, R.I. Masel, J. Power Sources 139 (2005) 15–20.
[7] R. Parsons, T. VanderNoot, J. Electroanal. Chem. 257 (1988) 9–45.
[8] X. Wang, J.-M. Hu, I.-M. Hsing, J. Electroanal. Chem. 562 (2004) 73–80.
[9] Y.-W. Rhee, S.Y. Ha, R.I. Masel, J. Power Sources 117 (2003) 35–38.
[10] K.-J. Jeong, Unpublished Results, Korea Institute of Science and Technology, 2006.
[11] H. Chang, I. Song, Song in Small Fuel Cells Conference, Washington, DC, April 2–4, 2006.
[12] S. Ha, C.A. Rice, R.I. Masel, A. Wieckowski, J. Power Sources 112 (2002) 655–659.
[13] D. Dunn-Rankin, E.M. Leal, D.C. Walther, Prog. Energy Combust. Sci. 31 (2005) 422–465.
[14] Y. Zhu, S.Y. Ha, R.I. Masel, J. Power Sources 130 (2004) 8–14.
[15] H. Dohle, J. Divisek, J. Mergel, H.F. Oetjen, C. Zingler, D. Stolten, J. Power Sources 105 (2002) 274–282.
[16] V. Gogel, T. Frey, Z. Yongsheng, K.A. Friedrich, L. Jorissen, J. Garche, J. Power Sources 127 (2004) 172–180.
[17] J.H. Ryu, S.M. Cho, The Fourth Asia-Pacific Chemical Reaction Engineering Symposium, vol. 4, 2005, pp. 397–398.
[18] P. Argyropoulos, K. Scott, W.M. Taama, J. Power Sources 87 (1999) 153–161.
[19] P. Argyropoulos, K. Scott, W.M. Taama, Electrochim. Acta 45 (1999) 1983–1998.
[20] J. Liu, Z. Zhou, X. Zhao, Q. Xin, G. Sun, B. Yi, PCCP 6 (2004) 134–137.
[21] M. Fowler, J.C. Amphlett, R.F. Mann, B.A. Peppley, P.R. Roberge, J. New Mater. Electrochem. Syst. 5 (2002) 1–7.
[22] M. Fowler, R.F. Mann, J.C. Amphlett, B.A. Peppley, P.R. Roberge, J. Power Sources 106 (2002) 274–283.
[23] S.Y. Ahn, S.J. Shin, H.Y. Ha, S.A. Hong, Y.C. Lee, T.W. Lim, I.H. Oh, J. Power Sources 106 (2002) 295–303.
[24] A.A. Kulikovsky, H. Scharmann, K. Wippermann, Electrochem. Commun. 6 (2004) 75–82.
[25] C. Xie, J. Bostaph, J. Pavio, J. Power Sources 136 (2004) 55–65.
[26] J.-H. Choi, K.-J. Jeong, Y. Dong, J. Han, T.-H. Lim, J.-S. Lee, Y.-E. Sung, J. Power Sources (2006).
[27] X. Ren, S. Gottesfeld, US Patent 6, 488, 837 (2002).